# An Investigation of the Ideal Reaction Conditions for Optimal Carbon Dioxide Absorption using Amino Acid Salt Solutions

Maansi Shroff

**Abstract**

Carbon dioxide ($CO_2$) is one of the most prominent greenhouse gases in the atmosphere and has been implicated in global temperatures. Post-combustion carbon capture (PCC) has been recognized to reduce $CO_2$ emissions from fossil fuel combustion sources. Chemical absorption is a popular type of PCC that utilizes reversible reactions to absorb $CO_2$. Common solvents are amine-based, but due to several disadvantages, amino acid salt solutions (AAS) are currently being examined. Amino acid molecules react with $CO_2$ to form carbamates and bicarbonate. Reaction ensemble Monte Carlo simulations (RxMC) were used to investigate amino acid solutions of glycine, lysine, proline, alanine, and glutamate under varying conditions of concentration, $CO_2$ loading, and temperature. The RxMC method samples these reactions in order to determine the equilibrium distribution of various solutions, which were then analyzed. Generally, higher concentration and $CO_2$ loading trials indicated more absorption. The temperature trials had less conclusive results, but the AAS displayed relatively high performance at high temperatures. Optimal simulations were run in order to verify these results. A glutamate solution at a 0.9 weight percentage concentration had the greatest $CO_2$ absorption. This study provided greater information regarding optimal conditions for maximum $CO_2$ absorption, as it would allow for an ultimate identification of the ideal solution to be implemented in power plants.

**Background**

The world currently faces the pressing issue of global warming and increased greenhouse emissions. Carbon dioxide ($CO_2$) is the most common one given its prominence in the atmosphere, especially due to the combustion of fossil fuels for transportation and electricity.[1] In 2018, the International Energy Agency discovered that $CO_2$ emissions from combustion were directly linked to over 0.3°C of each 1.0°C increase in global average annual surface temperatures.[2] To reduce emissions, researchers often use post-combustion capture (PCC), the most commonly used technique of carbon capture and storage technology.[1] PCC is responsible for absorbing 80-90% of $CO_2$ emissions from fossil fuel-fired power plants.[3] Is it the most practical and economical approach to absorb $CO_2$ since it would not require extensive measures to be implemented into current power plants.[4]

Many scientists utilize chemical PPC, which implements reversible chemical reactions with $CO_2$. Amine solutions, typically derived from ammonia, are effective at absorbing the molecule.[4] Unfortunately, they have high volatility, high oxidative degradation, deficiency at high temperatures, and produce toxic byproducts.[3,5] An ideal $CO_2$ absorbent would be efficient at high temperatures and have low volatility, little oxidative degradation, high $CO_2$ capture capacity, and be environmentally friendly.[4] Performance at high temperatures is especially important as flue gases, the combustion exhaust gases at power plants, can have temperatures of approximately 313 K when interacting with absorbent solvents as they cool.[5] Because amine solutions lack some of these characteristics, scientists are searching for a replacement. Given their low volatility, ensuring that less solvent would be lost to the atmosphere upon desorption, and heightened resistance to oxidative degradation, amino acid salt solutions (AAS) are attractive prospects for $CO_2$ capture.[1,6] Even better, AAS are naturally occurring.[1] Researchers hope to show that the remaining ideal properties exist.

Computational chemistry has allowed for investigation of these solutions. Computer models are simulated to view chemical reactions and determine molecular properties using thermodynamics and quantum mechanisms. Monte Carlo (MC) simulations are often performed, in which time is not a variable.[4] Instead, they make random moves of the particles, including translations and rotations, creating snapshots of the reaction. Within MC, the reaction ensemble Monte Carlo method (RxMC) informs about the equilibrium state of chemically reacting systems, including solutions at extreme conditions.[7–9] Due to ambiguity of the reaction mechanism between amino acids and $CO_2$, the RxMC method is favored because it can be unknown. The output gives equilibrium concentrations of molecules and average properties of the system.[9] Through computational chemistry, researchers can test theories about $CO_2$ and amino acid reactions, including the impact of extreme conditions, more efficiently and inexpensively than if done experimentally.[7]

This research uses RxMC simulations of single amino acid solutions to investigate how amino

acid concentration in water, $CO_2$ loading, and temperature can affect $CO_2$ absorption. Amino acid instead of AAS solutions are examined, but the properties that are deduced can be applied to AAS because the amine group, rather than the cation of the salt, interacts with $CO_2$. The study anticipates that increasing concentrations of the amino acid will result in greater absorption. Furthermore, the research will observe the ability of amino acids to absorb $CO_2$ as the loadings increase. A $CO_2$ loading refers to the ratio of $CO_2$ moles to amino acid moles in the solution.[10] Finally, prior research that considered temperature primarily viewed amines in a laboratory setting, testing only up to approximately 308 K.[11,12] Moreover, as aforementioned, amine solutions are inefficient at high temperatures, but this study expects to show that AAS can be more effective. The study hopes to see decreases in the equilibrium concentrations of $CO_2$.

By assessing how each amino acid interacts with $CO_2$ at various reaction conditions, the research plans to identify the optimal conditions for maximum $CO_2$ absorption, and ultimately decide which ideal absorbent solutions should be implemented in power plants.

**Procedure**

The RASPA 2.0 Software program was utilized to code the RxMC simulations.[8,9] Within the simulated solutions, $CO_2$, water ($H_2O$), hydronium ($H_3O^+$), and bicarbonate ($HCO_3^-$) could be found. Moreover, five amino acids – glycine, lysine, proline, alanine, and glutamate – were selected, as they are a representative sample of the standard amino acids.

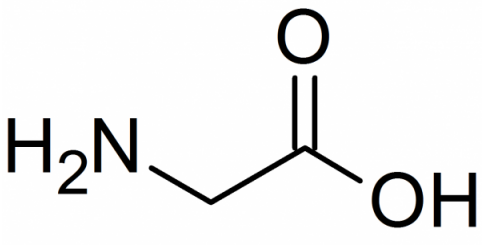


**Fig. 1.** Glycine structure.[13]

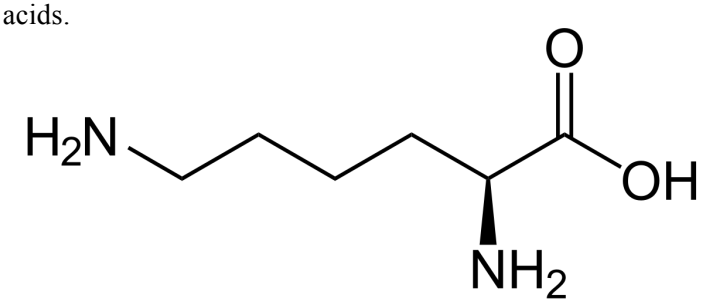


**Fig. 2.** Lysine structure.[13]

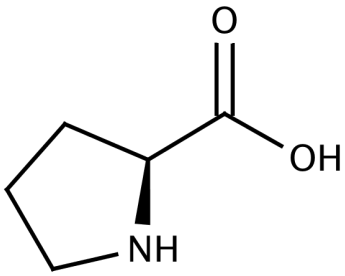


**Fig. 3.** Proline structure.[13]

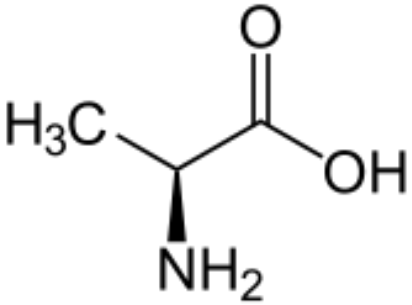


**Fig. 4.** Alanine structure.[13]

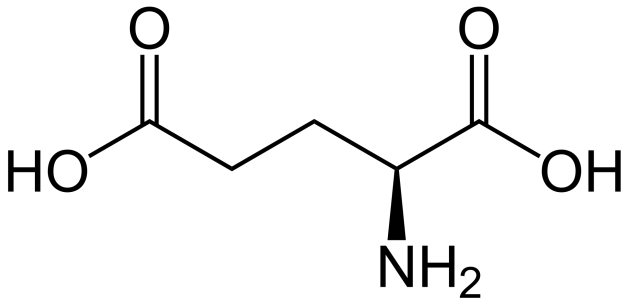


**Fig. 5.** Glutamate structure.[13]

The amino acids have the same general structure with an alpha carbon bonded to a carboxylic acid group ($COOH^-$) and an amino group ($NH_2$). Their differing side chains provide individual characteristics. Glycine is the smallest amino acid with hydrogen for its side chain, lysine is basic due to the extra basic amino group, proline has a secondary amine due to its ring structure, alanine has a methyl functional group, and glutamate has an extra carboxylic acid group, making it acidic. Additionally, each amino acid had an active, protonated, and carbamate form. In the active form, the amino and acid groups are deprotonated, but the protonated form has the amino group as protonated. The carbamate form has an added acid group from the carbon dioxide, and it is typically the product of the active form and $CO_2$. Below are structural examples of the active, protonated, and carbamate forms of glycine.

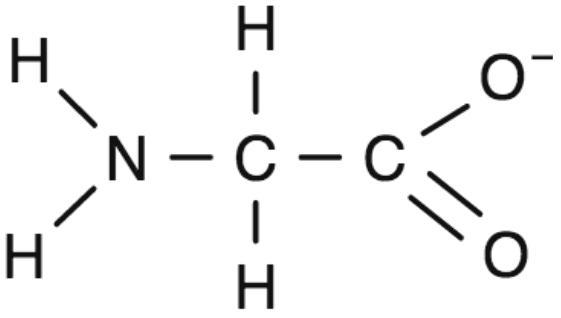


**Fig. 6.** Active form of glycine.

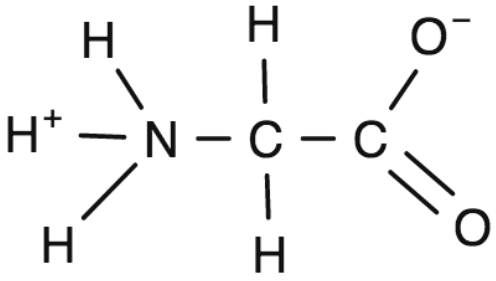


**Fig. 7.** Protonated form of glycine.

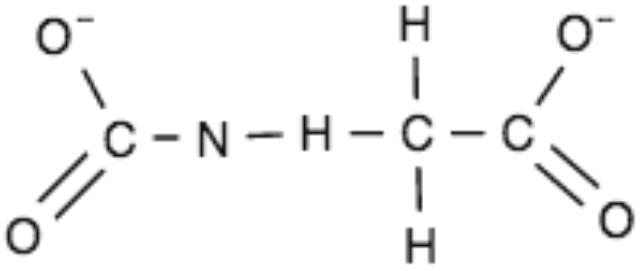


**Fig. 8.** Carbamate form of glycine.

Prior to creating code, scales for amino acid concentration, $CO_2$ loading, and temperature trials were determined. The concentration domain was 0.3 wt %, 0.6 wt %, and 0.9 wt %, while the temperature

was 298.15 K (room temperature) and a $CO_2$ loading of 50%. The unit of measurement, weight percentage, represented the fraction, instead of the percentage, of the total mass that the amino acids comprised. Although not in the domain, calculations were made at 0.5 wt %. It served as a constant value when testing other factors since each amino acid had at least ten molecules, making division simpler for the $CO_2$ loading trials. $CO_2$ loading was examined at 25%, 50%, 75%, 100%, and 125%. The constants were 0.5 wt % and 298.15 K. Lastly, temperature was tested from 298.15 K to 348.15 K at 10 degree Kelvin increments, with constants of a 0.5 wt % concentration and 50% $CO_2$ loading.

The numbers of $H_2O$, amino acid, and $CO_2$ molecules were calculated for each job. $HCO_3^-$, and the protonated and carbamate forms of amino acids had zero initial molecules. $H_3O^+$ molecules balanced charge and were in an equal ratio to all active forms of amino acids except glutamate. The active glutamate form has a -2 rather than -1 charge, so there were twice as many $H_3O^+$ molecules as active glutamate molecules. To find the number of active amino acid molecules at each concentration, the $H_2O$ molecules were fixed at 100 $H_2O$ molecules. Next, the molar masses of $H_2O$ and the amino acid in the calculation were determined. The number of amino acid molecules was solved with

$$Amino\ Acid\ Concentration\ (wt\%) = \frac{X_m\ (\frac{M_x}{N_A})}{X_m\ (\frac{M_x}{N_A}) + Y_m\ (\frac{M_x}{N_A})} \quad (1)$$

where $N_A$ is Avogadro's number at 6.022 x $10^{23}$ molecules per mole, $X_m$ is the number of amino acid molecules, $M_x$ is the molar mass of the amino acid molecule in grams per mole, $Y_m$ is the number of water molecules, and $M_y$ is the molar mass of a water molecule in grams per mole.

The calculated $X_m$ had to be a whole number since the reaction could not use a fraction of a molecule. So, if the last digit was five or larger, the molecules were rounded up. To find the number of $CO_2$ molecules, the unrounded $X_m$ was divided by two, since the loading is 50%, and rounded to a whole number. For $CO_2$ loading trials, the unrounded $X_m$ from a 0.5 wt % concentration was found and plugged into

$$CO_2\ Loading\ (\%) = \frac{Z_m}{X_m}\ x\ 100 \quad (2)$$

where $Z_m$ represents number of $CO_2$ molecules. $Z_m$ was rounded. For the temperature trials, the values from a 0.5 wt % concentration with a 50% $CO_2$ loading were used.

To run RASPA RxMC jobs, pre-defined molecule definition, force field, and pseudo-atom files were called.[7] Molecule definition specified the structure, force fields referred to van der Waals forces using the Lennard-Jones potential, and the pseudo-atom files explained the partial charges of each atom in the molecules. In addition, a pre-defined simulation file was used, where the initial concentrations were entered. To alter temperature, the value listed at the ExternalTemperature method was changed.

To represent the system, the RxMC method created a box. At the method BoxLengths, the dimensions were set to 25 by 25 by 25, unless there were more than 100 molecules of any substance. Here, the box dimensions were increased by five on each side. Before the job began, molecules were randomly inserted into the box to ensure that was no overlap. Even if this process failed, the job continued to run. To avoid this issue, the job's simulation folder was periodically checked to ensure that output folders were created. If they were not, the job was cancelled, the BoxLengths values were all increased by five units, and the simulation was re-submitted.

The RxMC method was coded to complete 1,000 initialization cycles and 20,000 production cycles. The initialization runs generated a mixture of the molecules. During the production runs, the RxMC method accounted for three reactions between $CO_2$ and an amino acid. Equations 3-5 used glycine as an example. $Glycine_a$ is active, $glycine_p$ is protonated, and $glycine_c$ is carbamate. $H_3O^+$ molecules, not shown, are present on both. The reactions reduced $CO_2$ by converting it to $HCO_3^-$ and carbamate forms using amino acids. This occurred directly in Equation 3, showing carbamate formation, and Equation 5, base-catalyzed bicarbonate formation. Depending on the stability of the carbamate, Equation 4 displayed how carbamate can hydrolyze to create $HCO_3^-$ and the active form of the amino acid.

$$CO_2 + 2\ glycine_a^{-1} \leftrightarrow\ glycine_p +\ glycine_c^{-2} \tag{3}$$

$$H_2O +\ glycine_c^{-2} \leftrightarrow glycine_a^{-1} + HCO_3^{-1} \tag{4}$$

$$CO_2 +\ H_2O +\ glycine_a^{-1} \leftrightarrow HCO_3^{-1} +\ glycine_p \tag{5}$$

RxMC randomly selected a reaction and a forward or reverse direction during each production run. The simulation then randomly removed either reactants or products and inserted the opposite molecules into the system to test whether thermodynamic properties were satisfied.[7] If the acceptance algorithm was fulfilled, the RxMC continued using the move to eventually reach equilibrium. However, if the algorithm failed, RxMC re-randomized the reaction and repeated the process. The simulation returned histogram values of the equilibrium concentrations. The mole fractions of the initial and equilibrium states were calculated. The mole fraction signified how much of a solution the molecule comprised. The active and carbamate forms of the amino acid, bicarbonate, and $CO_2$ were most important in determining $CO_2$ absorption capacity, so mole fractions were calculated for them. To calculate the initial mole fraction ($I_{mf}$), the number of reactant molecules were summed and the formula

$$I_{mf} = \frac{M_i}{T_i} \tag{6}$$

was used, where $M_i$ is the number of molecules of a substance in the initial state and $T_i$ is total number of initial molecules. For the equilibrium mole fraction ($E_{mf}$), the equation

$$E_{mf} = \frac{M_e}{T_e} \tag{7}$$

was utilized, where $M_e$ is the number of molecules of a substance in the equilibrium state and $T_e$ is total number of equilibrium molecules.

The mole fractions identified solutions with low $CO_2$. The mole differences (*md*) between the $E_{mf}$ and $I_{mf}$ were then computed through subtraction. Some solutions were shifted towards the reactants, meaning that the $E_{mf}$ in $CO_2$, and sometimes the active amino acid, increased. However, when the *md* for $CO_2$ was negative, it signified $CO_2$ had been absorbed. Thus, the *md* served to compare solutions, despite their varying initial concentrations, by isolating those where $CO_2$ was reduced. Based on the findings, optimal simulations with the most efficient values of concentration, $CO_2$ loading, and temperature were run, chosen based on where the largest negative mole differences for $CO_2$ were. To reaffirm the results, the percent decrease (*% dec*) for $CO_2$ was computed for trials that indicated absorption of $CO_2$ by plugging into

$$\% \, dec = \frac{md}{I_{mf}} \tag{8}$$

using the $I_{mf}$ of $CO_2$. This checked whether the largest mole differences corresponded with the largest percent decreases. Using all of the information determined, the most effective trial was identified. Excel created visual representations of the results.[14]

**Results and Discussion**

The $CO_2$ *md* ($E_{mf}$ - $I_{mf}$) were computed for each reaction and organized into Table 1 to identify trends in conditions. A positive value signified that the $CO_2$ $E_{mf}$ was larger than the $I_{mf}$, which happened when the reaction favored the reactants, considered unfavorable. This study searched for solutions with negative differences, as this meant that the $CO_2$ was absorbed. A large negative difference meant that the solution had high capture capacity.

Table 1: $CO_2$ *md* for All Trials and Amino Acids

| **$CO_2$ Mole Differences** | **Glycine** | **Lysine** | **Proline** | **Alanine** | **Glutamate** |
|---|---|---|---|---|---|
| **Concentration (wt %)** | -- | -- | -- | -- | -- |
| **0.3** | 0.00698 | 0.00995 | 0.00293 | 0.00831 | 0.00866 |
| **0.6** | -0.00128 | -0.00255 | 0.0027 | 0.00172 | -0.00831 |
| **0.9** | -0.00309 | -0.00374 | -0.00539 | -0.00625 | -0.03643 |
| **$CO_2$ Loading (%)** | -- | -- | -- | -- | -- |
| **25** | 0.00059 | 0.00949 | 0.00203 | 0.00694 | 0.00107 |
| **50** | 0.00109 | 0.00579 | 0.00383 | -0.00308 | 0.00204 |
| **75** | -0.0079 | 0.00239 | 0 | -0.01203 | -0.00815 |
| **100** | -0.00688 | -0.00074 | -0.00869 | -0.01025 | -0.00684 |
| **125** | -0.01012 | -0.00362 | -0.00658 | -0.00866 | -0.01596 |
| **Temperature (K)** | -- | -- | -- | -- | -- |
| **298.15** | 0.00109 | 0.00579 | 0.00383 | 0.0023 | 0.00204 |
| **308.15** | 0.00109 | 0.00579 | -0.00193 | -0.00853 | 0.00204 |
| **318.15** | 0.00109 | 0.00579 | 0.00383 | 0.0023 | 0.00204 |
| **328.15** | -0.00907 | 0.00579 | -0.00193 | 0.0023 | -0.00373 |
| **338.15** | 0.00109 | -0.0007 | -0.00193 | -0.00308 | -0.00373 |
| **348.15** | 0.00109 | 0.00579 | -0.00193 | -0.00853 | 0.00204 |
| **Optimal Simulation** | -- | -- | -- | -- | -- |
| **Concentration (wt%)** | 0.9 | 0.9 | 0.9 | 0.9 | 0.9 |
| **$CO_2$ Loading (%)** | 125 | 125 | 100 | 75 | 125 |
| **Temperature (K)** | 328.15 | 338.15 | **308.15**, 348.15 | **308.15**, 348.25 | **328.15**, 338.15 |
| **Calculated $CO_2$ *md*** | -0.00736 | -0.01226 | -0.01088 | -0.00555 | -0.00647 |

A 0.3 wt % amino acid concentration was not optimal since all *md* were positive. Glycine, lysine, and glutamate had negative differences at a 0.6 wt %, but the magnitudes of each *md* at a 0.9 wt % concentration were greater. As the concentration increased, the absorption tended to increase as well. In terms of trends in $CO_2$ loading, it appeared that the solutions had greater capture capacity above 50%. At 50%, only alanine had a negative *md*, but at 75%, 100%, and 125%, the majority of amino acids indicated $CO_2$ absorption. Thus, when more $CO_2$ molecules were present in the initial solution, the reaction yielded better results. Finally, the solutions appeared to absorb more $CO_2$ as the temperature increased, along each amino acid had its own individual trend. At 298.15 K, all *md* were positive, but decreases appeared at 308.15 K, 328.15 K, 338.15 K, and 348.15 K. 338.15 K had negative *md* for 80% of the amino acids. The results suggested that AAS solutions can perform fairly well at high temperatures, since each amino acid had an optimal temperature within the range of 328.15 K and 348.15 K.

The optimal jobs were run with the conditions listed in Table 1. Specific input and output values can be found in Table 3 of the Appendix. The optimal jobs were one of the few trials where all five amino acids absorbed $CO_2$, as indicated by the negative *md*. The active amino acid forms also decreased in all optimal trials, evidenced by Table 3. These trials all absorbed $CO_2$ and had combinations of the three factors, so it is possible that solutions with varying levels could hold higher carbon capture capacity. The optimal *md* for lysine and proline were the largest of their respective trials.

As seen in Table 1, the most efficient trials for each amino acid were identified based on where the largest negative $CO_2$ *md* were. When there were multiple trials with the same *md*, the *md* in $HCO_3^-$, the active amino acid, and carbamate form were examined using Fig. 13 - 28 in the Appendix. Ideally, the active form would decrease, primarily because it is a reactant in Eq. 3 and Eq. 5. However, it can increase if the simulation utilized Eq. 4. On the other hand, bicarbonate and the carbamate forms should have large increases. In some of the temperature trials, all four *md* values were equivalent. In those cases, the $E_{mf}$ concentrations were graphed, but because each amino acid's temperature trials had the same initial concentrations, the $E_{mf}$ were also equal in those simulations. In that situation, the lower temperature, bolded in Table 1, was considered optimal, as it would be least costly to implement in a power plant. To check that these conditions were correct, the *% dec* in $CO_2$ was determined. Fig. 9 indicates the *% dec* for all trials that had a negative $CO_2$ *md*.

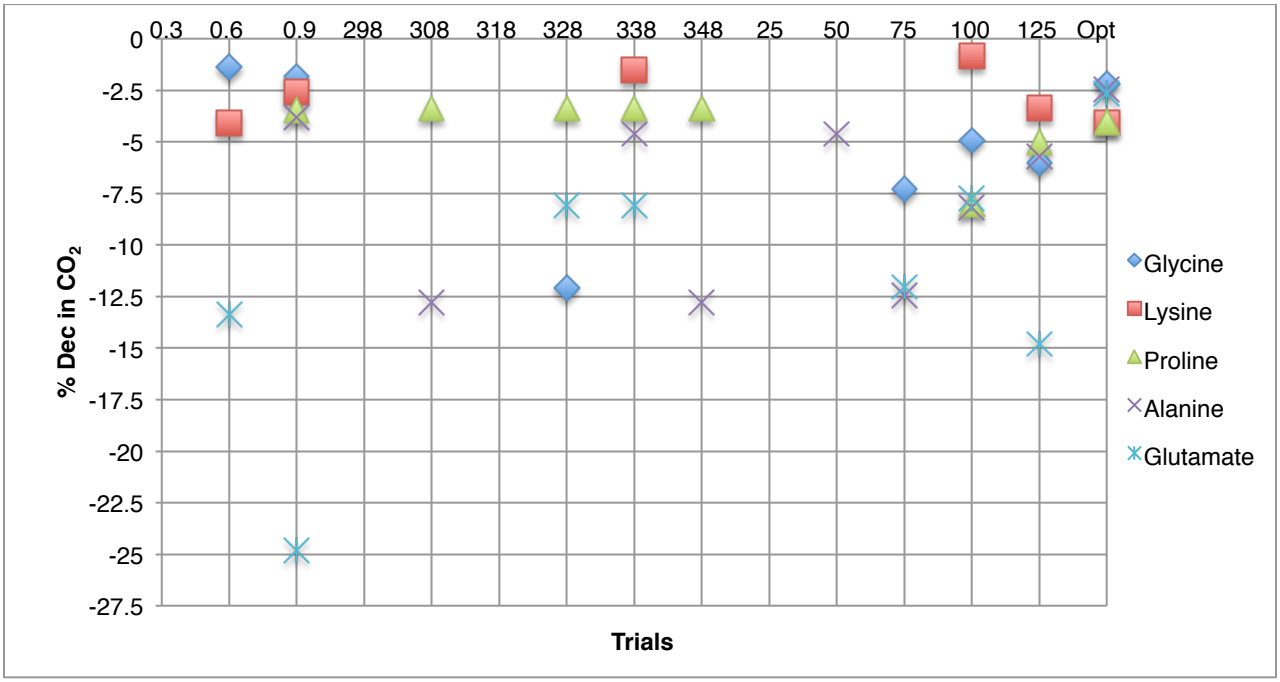


**Fig. 9.** Percent Decreases in Trials with $CO_2$ Absorption.

From this plot, alanine indicated absorption occurring 60% of the trials, while proline and glutamate performed it only 53.3% of the time. However, glutamate solutions tended to have higher absorption

percentages than other amino acids. In addition, although Table 1 indicated that the optimal trials had greatest negative *md* for lysine and proline, this figure showed that the *% dec* was not the lowest for their respective trials. Instead, the 0.6 wt % lysine solution absorbed more $CO_2$. Moreover, proline with 100% and 125% loadings were more effective than the optimal trial. According to these results, a solution could possess a large negative difference solely because they had large initial concentrations in molecules like $CO_2$. However, that did not necessarily mean that it reduced $CO_2$ emissions at the greatest degree.

From Fig. 9, the optimal trials for proline, alanine, and glutamate were confirmed as their conditions matched the largest negative *md* in $CO_2$ for those factors. However, glycine and lysine have variability in their conditions between Table 1 and Fig. 9, since the figure suggested that the glycine solution at a 75% loading had greater absorption than at 125%. To determine the most optimal trial for glycine, Fig. 10 was generated.

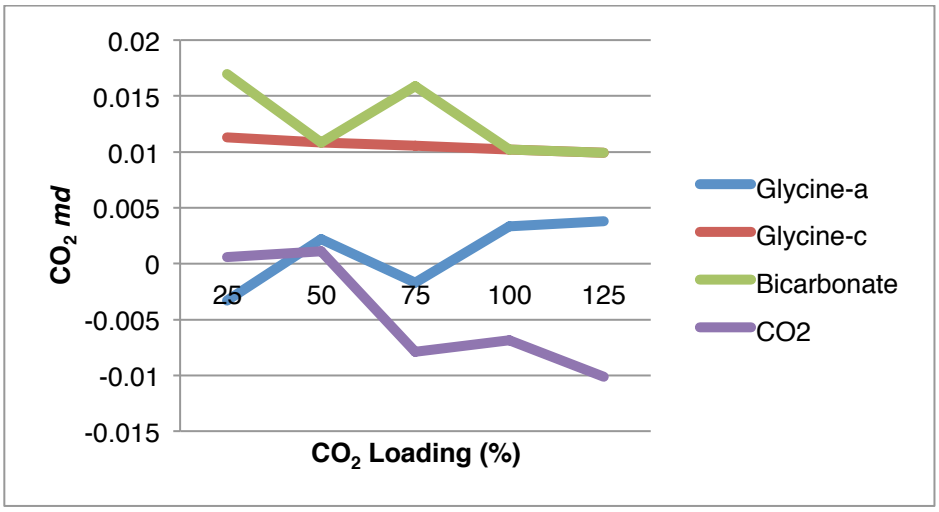


**Fig. 10.** Graph of *md* during glycine reaction simulations at various $CO_2$ loadings.

At a 125% loading, the $CO_2$ *md* was the lowest, but $glycine_a$ increased and $HCO_3^-$ and $glycine_c$ were not at their peak increases. Eq. 4 explains the increase in $glycine_a$. However, at a 75% loading, $CO_2$ and $glycine_a$ were decreasing. In addition, $HCO_3^-$ at its peak increase, and $glycine_c$ increased more that in the 125% loading solution. These properties were more favorable, so this evidence suggested the 75% loading was more optimal. As a result, a second optimal glycine trial was generated with a 0.9 wt % concentration, loading of 75%, and temperature of 328.15 K.

Fig. 10 also displayed that the 0.6 wt % lysine solution was more successful at reducing $CO_2$ emissions than the 0.9 wt % solution. To test what the true optimal concentration for lysine was, Fig. 11 was created.

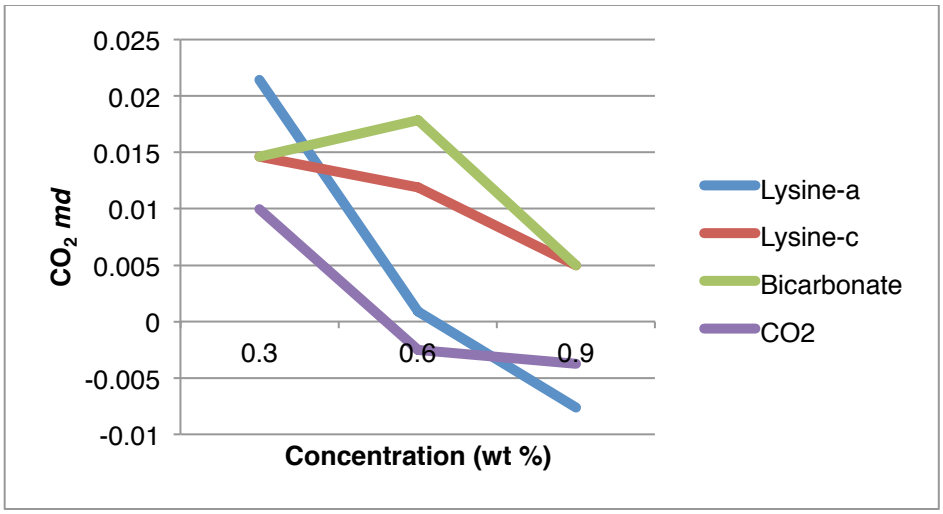


**Fig. 11.** Graph of *md* during lysine reaction simulations at various concentrations.

At a 0.9 wt % concentration, the lysine solution had the lowest $CO_2$ and $lysine_a$ *md*. However, $HCO_3^-$ and $lysine_c$ were at their lowest *md*. At the 0.6 wt %, the $CO_2$ *md* was negative, and the $lysine_a$, $HCO_3^-$, and $lysine_c$ had positive *md*. $HCO_3^-$, and $lysine_c$ were at their highest points. Another optimal lysine simulation was run with a 0.6 wt %, 125% loading, and 338.15 K. Using the revised optimal trials, with initial and equilibrium values in Table 4 of the Appendix, Fig. 4 was created to show the updated *% dec* in $CO_2$.

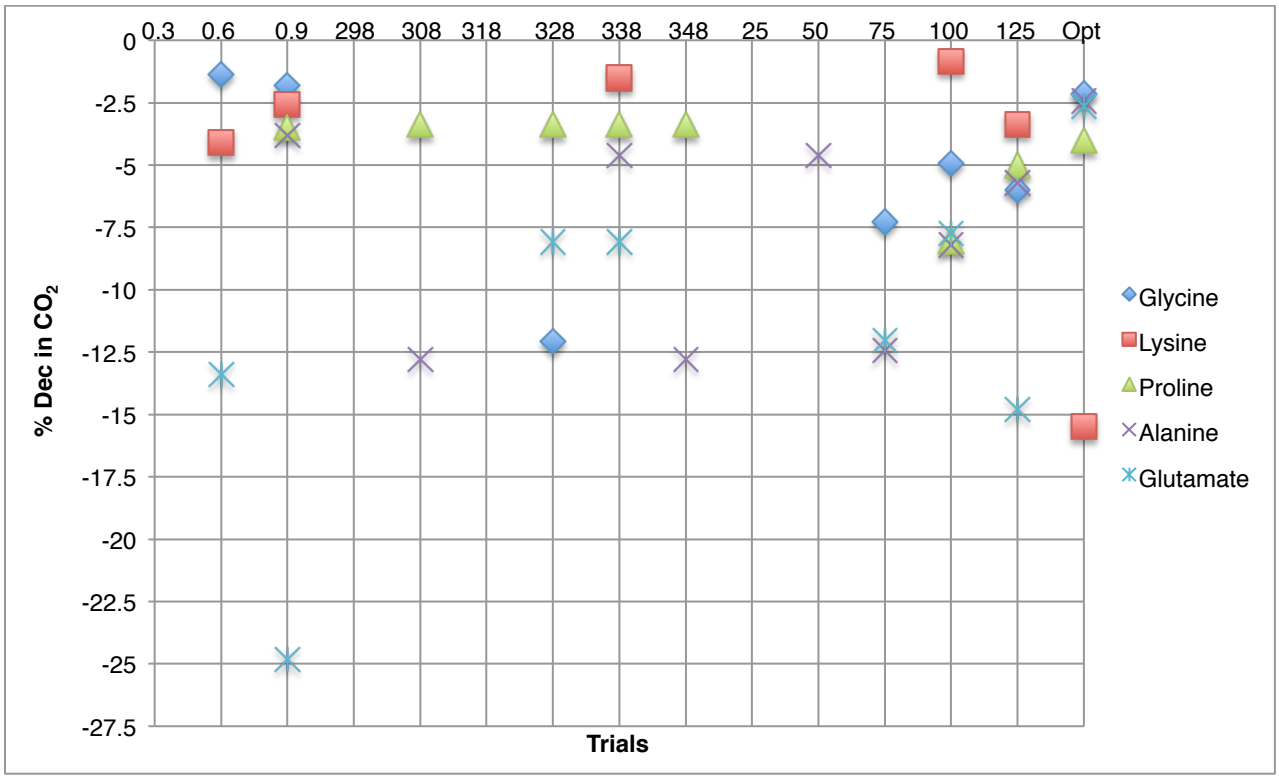


**Fig. 12.** Revised Percent Decreases in Trials with $CO_2$ Absorption.

In Fig. 12, the new percent decreases for the revised optimal glycine and lysine trials can be seen. Glycine has almost the exact same absorption, but the lysine solution increased its absorption drastically. In fact, it has the second maximum absorption out of all the trials that reduced $CO_2$ concentration. Thus, the revised optimal trial for lysine proved to be more effective, suggesting that the combination of the three factors can result in more effective absorption.

From this Table 1, and Fig. 12, the most optimal conditions for an AAS solution were concluded. The glutamate trial at a 0.9 wt % concentration presented the most absorption. Important values related to its significance in this research are noted in Table 2.

Table 2: Significant Values of Glutamate Trial at 0.9 wt % Concentration

| Mean (mol) | Standard Deviation (mol) | Trial Value (mol) | Percent Decrease (%) | Z-Score | P-value |
|---|---|---|---|---|---|
| -0.00204 | 0.00736 | -0.03640 | -24.83894 | -4.67541 | 0.00097 |

The z-score and probability under the curve, also considered the p-value, were determined using Excel, under the assumption that the data set of $CO_2$ *md* was normally distributed, which was likely since its large size suggested a normal shape. The z-score conveys how many standard deviations from the mean a value is, and the p-value gives the probability of observing a value as extreme as that one within the data set. Typically, when a z-score is past ±3, it is outside 99.7% of the data. Here, a z-score close to -5 indicated a miniscule percentage of the data. The p-value stated that there was 0.097% likelihood of a solution absorbing 24.83894059% or more of the $CO_2$ in the solution. A p-value is generally considered significant when below 0.05, making this value is significant. So, this particular solution produced a decrease abnormally larger than other trials. Therefore, the glutamate solution had the greatest carbon capture abilities and can be considered to have the most optimal conditions, at a 0.9 wt % concentration, loading of 50%, and temperature of 298.15 K.

While strong results were determined, the design of the study encountered several obstacles. There were seventy-five simulations to run, and each had 1,000 initialization runs and 20,000 production runs. Therefore, each test took several days. As a result, the study was deterred from creating more complex solutions. Moreover, the RASPA program did not return errors before executing a job. This was a possible source of error, but the problem was controlled re-checking simulation inputs for inaccuracies numerous times prior to job submission.

**Conclusion**

As earlier stated, the five amino acids are a representative sample, but they are also common in certain strands of algae. In order to implement AAS solutions on campus power plants, one university uses algae and extracts the amino acids to form the solution. Thus, they wanted to compare the performance of those specific amino acids. However, future computational chemists should consider working with different ones, especially since this research determined that alanine and glutamate performed the best. In comparison to alanine, other amino acids with nonpolar alkyl groups like valine, leucine, and isoleucine could be examined. To parallel glutamate, aspartate, the other acidic amino acid, would be investigated.

In addition, researchers could go beyond the specified ranges and test higher or lower values of all three factors. Within those ranges, smaller intervals of concentration, temperature, and $CO_2$ loadings within the domains should be investigated. Examining more precise scales would provide greater insight. Moreover, a researcher ought to run more simulations with a combination of factors. Within this study, the constant values for various trials were 0.5 wt %, 50% loading, and 298.15 K. The optimal simulations modified all three factors, and lysine indicated the greatest percent absorption of $CO_2$ than any other trial. Thus, this suggests that varied constants could yield satisfactory results. In addition, proline, alanine, and glutamate had multiple optimal temperatures. Future simulations would examine the other temperatures to compare capture capacity between the solutions. Previous research has also suggested that AAS formed with multiple amino acids could reduce $CO_2$ emissions more rapidly and efficiently.[5] Further information would tell scientists if amino acid pairs are more effective at capturing $CO_2$ to reduce global warming. Different concentrations, temperatures, and $CO_2$ loadings could be assessed.

Based on the trends in $CO_2$ absorption, it appeared that all amino acid solutions tended to have higher capture abilities with increased concentrations. The Wilson Research Group is now running simulations using a 0.9 wt % concentration as that tended to indicate the most absorption. At lower $CO_2$ loadings, most amino acids had solutions with a shift towards the reactants. However, as the loadings increased, absorption occurred, particularly at 100% and 125%. Thus, the conclusion can be made that more initial amino acid and $CO_2$ molecules encouraged greater $CO_2$ absorption. The trends in temperature were less clear, so it would be beneficial to test more intervals and a greater range. However, flue gases are around 313 K when they react with capturing solvents, and every amino acid had optimal temperatures beyond that value. Some optimal trials were run at 308.15 K, but they were chosen instead of a higher temperature due to expected costs of implementation. Therefore, AAS solutions would be suitable for higher temperatures as they have carbon capture ability at those values. Currently, the glutamate solution with a 0.9 % wt concentration, temperature of 298.15 K, and $CO_2$ loading of 50% demonstrated the ability to absorb nearly 25% of the $CO_2$ in the solution. This research brings the

scientific community closer to a complete identification of the ideal reaction conditions of an AAS solution with $CO_2$. Now, the concentrations, loadings, and temperatures can be more focused in forthcoming simulations. Using that information, the exact AAS solution for a power plant will be known in the very near future.

## Figure Appendix

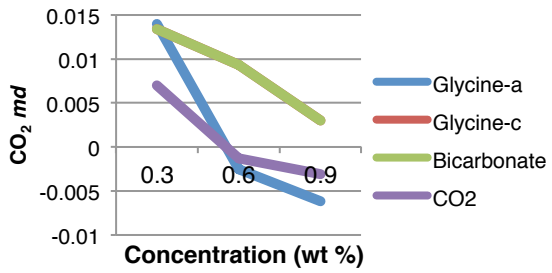


**Fig. 13.** Graph of *md* during glycine reaction simulations at various concentrations

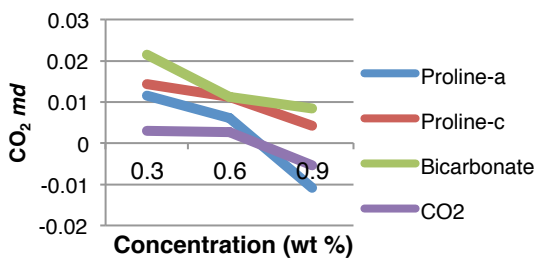


**Fig. 14.** Graph of *md* during proline reaction simulations at various concentrations.

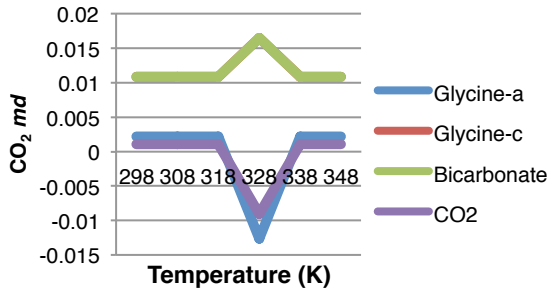


**Fig. 15.** Graph of *md* during glycine reaction simulations at various temperatures.

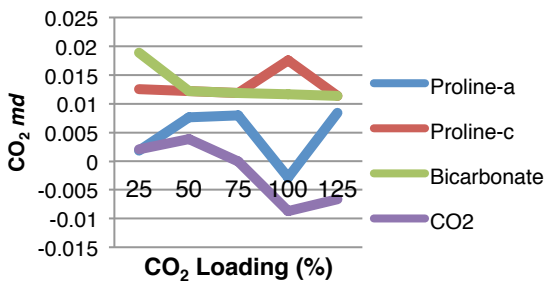


**Fig. 16.** Graph of *md* in proline reaction simulations at various $CO_2$ loadings.

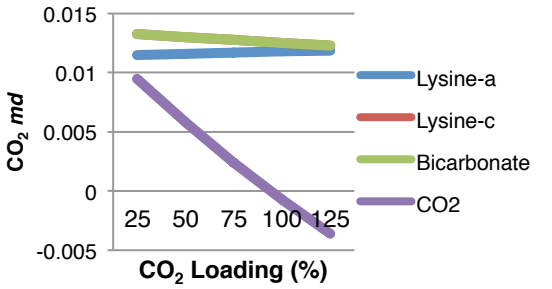


**Fig. 17.** Graph of *md* during lysine reaction simulations at various $CO_2$ loadings.

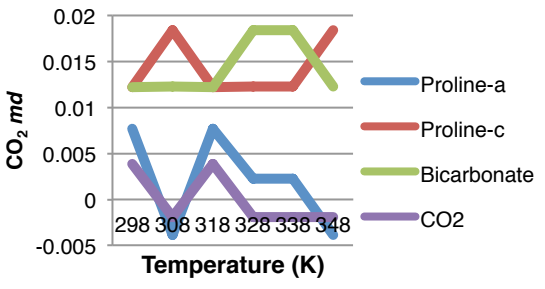


**Fig. 18.** Graph of *md* during proline reaction simulations at various temperatures.

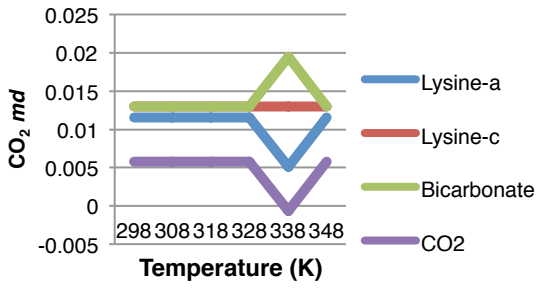


**Fig. 19.** Graph of *md* during lysine reaction simulations at various temperatures.

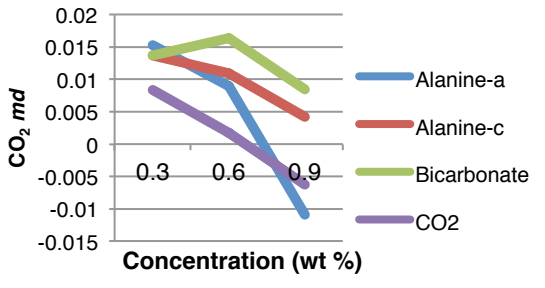


**Fig. 20.** Graph of *md* in alanine reaction simulations at various concentrations.

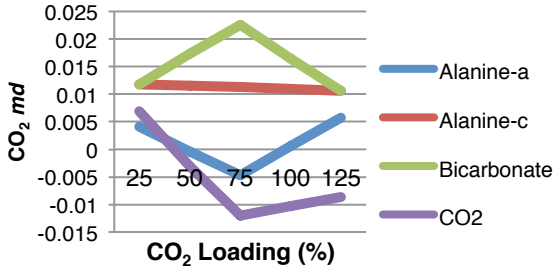


**Fig. 21.** Graph of *md* in alanine reaction simulations at various $CO_2$ loadings.

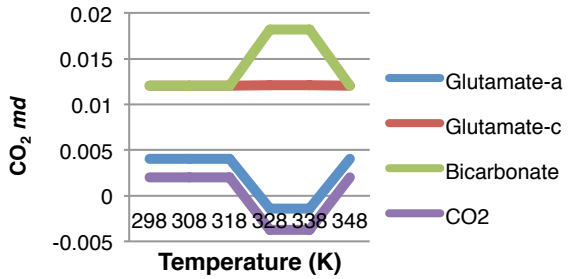


**Fig. 22.** Graph of *md* in glutamate reaction simulations at various temperatures.

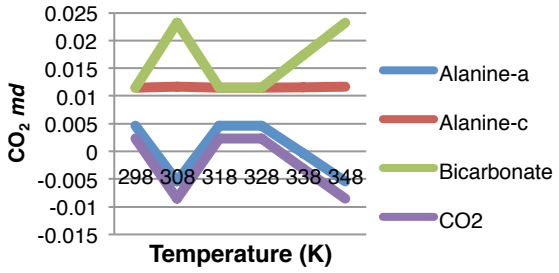


**Fig. 23.** Graph of *md* in alanine reaction simulations at various temperatures.

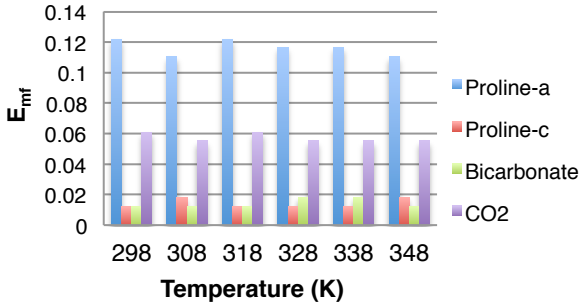


**Fig. 24.** Bar chart of critical $E_{mf}$ values during proline reaction simulations at various temperatures.

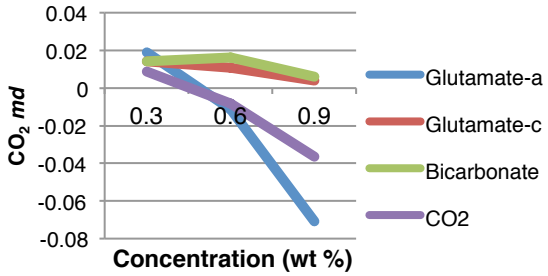


**Fig. 25.** Graph of *md* in glutamate reaction simulations at various concentrations.

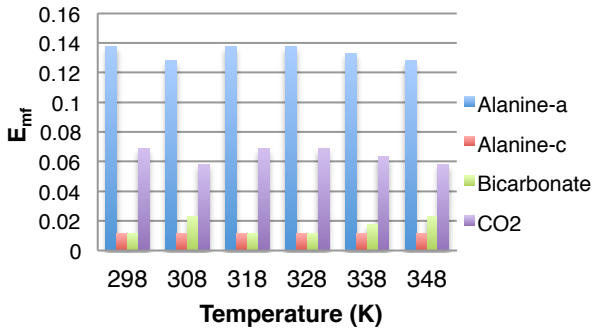


**Fig. 26.** Bar chart of critical $E_{mf}$ values during alanine reaction simulations at various temperatures.

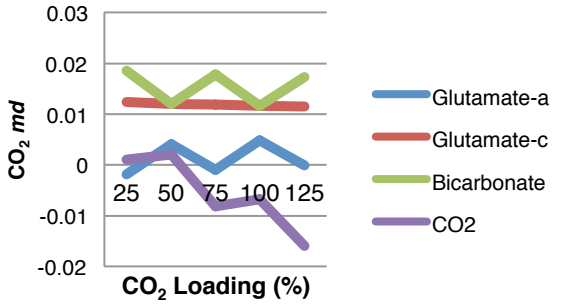


**Fig. 27.** Graph of *md* in glutamate reaction simulations at various $CO_2$ loadings.

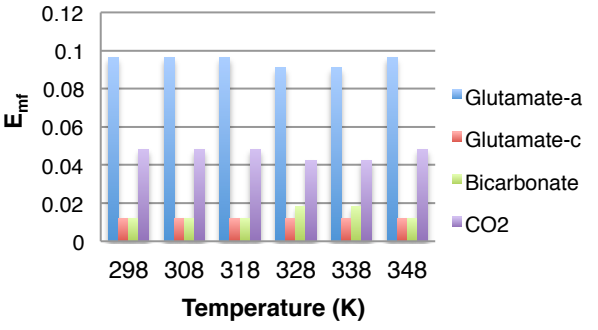


**Fig. 28.** Bar chart of critical $E_{mf}$ values during glutamate reaction simulations at various temperatures.

**Table Appendix**

Table 3: Initial and Equilibrium Values for Optimized Trials

| **Optimal Trial** | **Value** |
|---|---|
| Initial H2O | 100 |
| **Glycine** | --- |
| Initial Glycine-a | 216 |
| Imf Glycine-a | 0.26933 |
| Emf Glycine-a | 0.26634 |
| *md* Glycine-a | -0.00298 |
| Initial CO2 | 270 |
| Imf CO2 | 0.33666 |
| Emf CO2 | 0.3293 |
| *md* CO2 | -0.00736 |
| *md* Glycine-c | 0.00242 |
| *md* Bicarbonate | 0.00242 |
| **Lysine** | --- |
| Initial Lysine-a | 111 |
| Imf Lysine-a | 0.24078 |
| Emf Lysine-a | 0.23554 |
| *md* Lysine-a | -0.00524 |
| Initial CO2 | 139 |
| Imf CO2 | 0.30152 |
| Emf CO2 | 0.28926 |
| *md* CO2 | -0.01226 |
| *md* Lysine-c | 0.00413 |
| *md* Bicarbonate | 0.0062 |
| **Proline** | --- |
| Initial Proline-a | 141 |
| Imf Proline-a | 0.2696 |
| Emf Proline-a | 0.26055 |
| *md* Proline-a | -0.00905 |
| Initial CO2 | 141 |
| Imf CO2 | 0.2696 |
| Emf CO2 | 0.25872 |
| *md* CO2 | -0.01088 |
| *md* Proline-c | 0.0055 |
| *md* Bicarbonate | 0.0055 |
| **Alanine** | --- |
| Initial Alanine-a | 182 |
| Imf Alanine-a | 0.30283 |
| Emf Alanine-a | 0.2976 |
| *md* Alanine-a | -0.00523 |
| Initial CO2 | 137 |
| Imf CO2 | 0.22795 |
| Emf CO2 | 0.2224 |
| *md* CO2 | -0.00555 |
| *md* Alanine-c | 0.0032 |
| *md* Bicarbonate | 0.0032 |
| **Glutamate** | --- |
| Initial Glutamate-a | 110 |
| Imf Glutamate-a | 0.19366 |
| Emf Glutamate-a | 0.19257 |
| *md* Glutamate-a | -0.00109 |
| Initial CO2 | 138 |
| Imf CO2 | 0.24296 |
| Emf CO2 | 0.23649 |
| *md* CO2 | -0.00647 |
| *md* Glutamate-c | 0.00338 |
| *md* Bicarbonate | 0.00338 |

Table 4: Revised Initial and Equilibrium Values for Optimal Glycine and Lysine Trials

| **Glycine** | --- |
|---|---|
| Concentration (wt %) | 0.9 |
| Temperature (K) | 328.15 |
| CO2 Loading (%) | 75 |
| Initial Glycine-a | 216 |
| Imf Glycine-a | 0.31124 |
| Emf Glycine-a | 0.30641 |
| *md* Glycine-a | -0.00483 |
| Initial CO2 | 162 |
| Imf CO2 | 0.23343 |
| Emf CO2 | 0.22841 |
| *md* CO2 | -0.00502 |
| *md* Glycine-c | 0.00279 |
| *md* Bicarbonate | 0.00279 |
| **Lysine** | --- |
| Concentration (wt %) | 0.6 |
| Temperature (K) | 338.15 |
| CO2 Loading (%) | 125 |
| Initial Lysine-a | 18 |
| Imf Lysine-a | 0.11321 |
| Emf Lysine-a | 0.10556 |
| *md* Lysine-a | -0.00765 |
| Initial CO2 | 23 |
| Imf CO2 | 0.14465 |
| Emf CO2 | 0.12222 |
| *md* CO2 | -0.02243 |
| *md* Lysine-c | 0.01111 |
| *md* Bicarbonate | 0.02778 |

## References


(1) Zhang, Z.; Li, Y.; Zhang, W.; Wang, J.; Soltanian, M. R.; Olabi, A. G. Effectiveness of Amino Acid Salt Solutions in Capturing CO2: A Review. *Renew. Sustain. Energy Rev.* **2018**.

(2) IEA. *Global Energy and CO2 Status Report*; 2018.

(3) Wei, S. C. C.; Puxty, G.; Feron, P. Amino Acid Salts for CO2capture at Flue Gas Temperatures. In *Energy Procedia*; 2013. https://doi.org/10.1016/j.egypro.2013.05.134.

(4) Yang, X.; Rees, R. J.; Conway, W.; Puxty, G.; Yang, Q.; Winkler, D. A. Computational Modeling and Simulation of CO 2 Capture by Aqueous Amines. *Chemical Reviews*. 2017.

(5) Lerche, B. M. *CO2 Capture from Flue Gas Using Amino Acid Salt Solutions : Ph. D. Thesis*; DTU Chemical Engineering, Department of Chemical and Biochemical Engineering, 2012.

(6) Guo, D.; Thee, H.; Tan, C. Y.; Chen, J.; Fei, W.; Kentish, S.; Stevens, G. W.; Da Silva, G. Amino Acids as Carbon Capture Solvents: Chemical Kinetics and Mechanism of the Glycine + CO2 Reaction. *Energy and Fuels* **2013**. https://doi.org/10.1021/ef400413r.

(7) Turner, C. H.; Brennan, J. K.; Lisal, M.; Smith, W. R.; Karl Johnson, J.; Gubbins, K. E. Simulation of Chemical Reaction Equilibria by the Reaction Ensemble Monte Carlo Method: A Review. *Mol. Simul.* **2008**. https://doi.org/10.1080/08927020801986564.

(8) Dubbeldam, D.; Calero, S.; Ellis, D. E.; Snurr, R. Q. RASPA: Molecular Simulation Software for Adsorption and Diffusion in Flexible Nanoporous Materials. *Mol. Simul.* **2016**. https://doi.org/10.1080/08927022.2015.1010082.

(9) Dubbeldam, D.; Torres-Knoop, A.; Walton, K. S. On the Inner Workings of Monte Carlo Codes. *Mol. Simul.* **2013**. https://doi.org/10.1080/08927022.2013.819102.

(10) Kim, Y. E.; Lim, J. A.; Jeong, S. K.; Yoon, Y. Il; Bae, S. T.; Nam, S. C. Comparison of Carbon Dioxide Absorption in Aqueous MEA, DEA, TEA, and AMP Solutions. *Bull. Korean Chem. Soc.* **2013**. https://doi.org/10.5012/bkcs.2013.34.3.783.

(11) Simons, K.; Brilman, W.; Mengers, H.; Nijmeijer, K.; Wessling, M. Kinetics of CO2 Absorption in Aqueous Sarcosine Salt Solutions: Influence of Concentration, Temperature, and CO2 Loading. *Ind. Eng. Chem. Res.* **2010**. https://doi.org/10.1021/ie100241y.

(12) Littel, R. J.; Versteeg, G. F.; Van Swaaij, W. P. M. Kinetics of CO2 with Primary and Secondary Amines in Aqueous Solutions-I. Zwitterion Deprotonation Kinetics for DEA and DIPA in Aqueous Blends of Alkanolamines. *Chem. Eng. Sci.* **1992**. https://doi.org/10.1016/0009-2509(92)80319-8.

(13) Helmenstine, A. M. These Are the Amino Acid Structures. https://www.thoughtco.com/amino-acid-structures-4054180 (accessed Aug 16, 2019).

(14) Katz, A. Microsoft Excel 2010. *Style (DeKalb, IL)* **2010**. https://doi.org/10.1007/978-1-4302-2956-8.